

# Optimization of the current ramp-up phase for hybrid ITER discharges

G.M.D. Hogeweij<sup>1</sup>, J.-F. Artaud<sup>2</sup>, T.A. Casper<sup>3</sup>, J. Citrin<sup>1</sup>, F. Imbeaux<sup>2</sup>, F. Köchl<sup>4</sup>, X. Litaudon<sup>2</sup>, ITM-TF ITER Scenario Modelling group

<sup>1</sup> FOM-Institute for Plasma Physics Rijnhuizen, Association EURATOM-FOM, Trilateral Euregio Cluster, P.O.Box 1207, Nieuwegein, The Netherlands, [www.rijnhuizen.nl](http://www.rijnhuizen.nl)

<sup>2</sup> CEA, IRFM, F-13108 Saint Paul lez Durance, France

<sup>3</sup> ITER Organization, F-13115 Saint Paul lez Durance, France

<sup>4</sup> Association EURATOM-ÖAW/ATI, Atominstytut, TU Wien, 1020 Vienna, Austria

**1. Introduction.** During the current ramp-up phase of ITER MHD instabilities have to be avoided, flux consumption has to be minimized, and this has to be achieved within the narrow operational window of ITER. Ramp-up for the hybrid scenario moreover requires that the  $q$  profile is shaped:  $q_{\min}$  should stay near or slightly above 1 and, for an optimized fusion performance, the  $q$  profile should have the typical hybrid shape with a wide flat region [1]. This paper reports on a systematic effort to optimize the current ramp-up phase for the ITER hybrid scenario, and to assess the sensitivity of the results to the assumptions made. The aim is to arrive at an optimum  $q$  profile at the beginning of the current flat-top of  $\simeq 12$  MA, with minimum flux consumption, and staying within the ITER operational boundaries.

Validation on the ramp-up phase of JET, AUG and Tore Supra [2,3] has shown that both empirical scaling based models (H-mode scaling with H-factor  $H=0.4$ ; L-mode scaling with factor 0.6 gives the same result) and the semi-empirical Bohm/gyro-Bohm model (L-mode version, ITB shear function off) yield a good reproduction of this phase for considered discharges, in terms of  $T_e$  and  $q$  profile and  $l_i$ . Therefore these models have been used in the reported work, which was carried out with the CRONOS integrated suite of codes [4].

## 2. Assumptions made

Following assumptions for the baseline scenario were adopted from the ITER team:

(i) An expanding ITER shape is used, starting on the LFS of the torus, with initial plasma volume  $\simeq 50\%$  of the final plasma volume. X-point formation takes place after 15s, when  $I_p = 3.5$  MA.

(ii) A flat  $Z_{\text{eff}}$  profile is assumed, decreasing in time with increasing density, with an asymptotic value of 1.7 [5].

(iii) A rather low density of  $n_e = 0.25 \cdot n_e^{\text{Gw}}$  is taken.

The  $n_e$  profile is assumed to be parabolic with a moderate peaking factor  $n_e(0)/\langle n_e \rangle = 1.3$ . This is a compromise between the (unrealistic) flat  $n_e$  profile used by the ITER team and the peaking factor of  $\simeq 1.5$  predicted by scaling studies [6].

The total input power should stay below the L-H threshold during the whole ramp-up phase; for the reference case  $P_{\text{LHthr}} \simeq 29$  MW at end of the current ramp-up.

The  $I_p$  ramp rate is chosen such that  $I_p = 12$  MA is reached after 80 s. Other assumptions ( $T_{e,i}(\text{edge})$ , initial  $T_{e,i}$  and  $l_i$ ) are based on experimental evidence.

The simulations start 1.5 s after breakdown, when  $I_p = 0.5$  MA.

## 3. Choice of heating and current drive scheme

The ITER design and limitations used, e.g. the designed geometries of the heating systems are used; NBI is only allowed if  $\langle n_e \rangle \geq 2 \cdot 10^{19} \text{m}^{-3}$ ; NBI can only be applied at half or full power (i.e. 16.5 or 33 MW).

The logical way to get at the hybrid  $q$  profile is as follows: let the discharge evolve without additional heating until  $q(0)$  close to 1, and then apply off-axis heating and CD

to clamp  $q(0)$  and broaden the  $q$  profile. For the ramp-up parameters both ECRH from the equatorial launcher and ICRF deposit very centrally, so are unsuitable. Hence the remaining heating and CD options are: NBI (using the off-axis setting), LHCD and the Upper Port Launcher (UPL) of ECCD. The latter has 2 antennas with different ranges of poloidal angles, i.e. of power deposition radius ( $\rho_{dep}$ ). Table 1 gives an overview of the options.

CD method	$\rho_{dep}$	width	notes
UPL ECCD 1st antenna	$\geq 0.4$	narrow	depends on poloidal angle
UPL ECCD 2nd antenna	$\geq 0.6$	narrow	depends on poloidal angle
LHCD	0.3 - 0.6	narrow	depends on plasma parameters
off-axis NBI	0.3	wide	

Table 1: Overview of CD methods; the  $\rho_{dep}$  given here are for the plasma parameters during the  $I_p$  ramp-up phase.

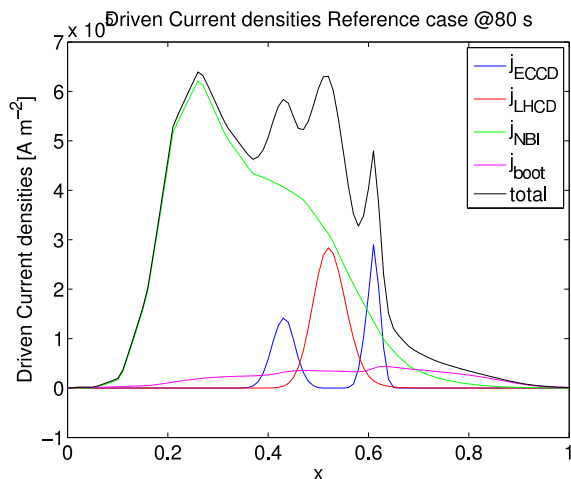


Figure 1: Example of driven current densities, using a balanced mix of sources, for the reference case at 80 s: 5 + 15 MW of ECCD from the two UPL antennas (blue), 4 MW of LHCD (red) and 16.5 MW of NBI (green). Also shown is the bootstrap current density (magenta) and the total non-inductive driven current density (black). Note that this is merely an example; since the total power significantly exceeds  $P_{LHthr}$ , this is not the power mix used in the remainder of this paper.

Since ECCD and LHCD have quite narrow power deposition profiles, excessive use of one of these as only current drive source would yield a very localized net CD profile, leading to locally a strong negative shear, which should be avoided because of the risk of triggering unwanted MHD. Therefore it is better to use a combination of CD sources in such a way that the CD is spread over a wide off-axis zone, thus compensating for the peaked ohmic drive. Figure 1 gives an example if this.

#### 4. Reference case

Figure 2 shows the optimized scenario, as sketched in the previous section, for the reference case, using the scaling model ( $H=0.4$ ), full lines) and using the Bohm-gyroBohm model (dashed lines). Figure 3 shows the profiles of  $T_{e,i}$  and  $q$  at the end of the  $I_p$  ramp-up. For reference the figures also show the result without any additional heating.

The Bohm-gyroBohm model predicts  $\sim 40\%$  lower temperatures than the scaling model, and therefore a faster current penetration; this is accounted for by switching on ECCD and LHCD 20 s earlier. As seen from fig.3 in both cases a good hybrid  $q$  profile is reached at the end of the ramp-up.

By post processing the simulation results with the FREEBIE [7] code it has been checked that the reference case, both with and without additional heating, is safely within the boundaries put by ITER coils.

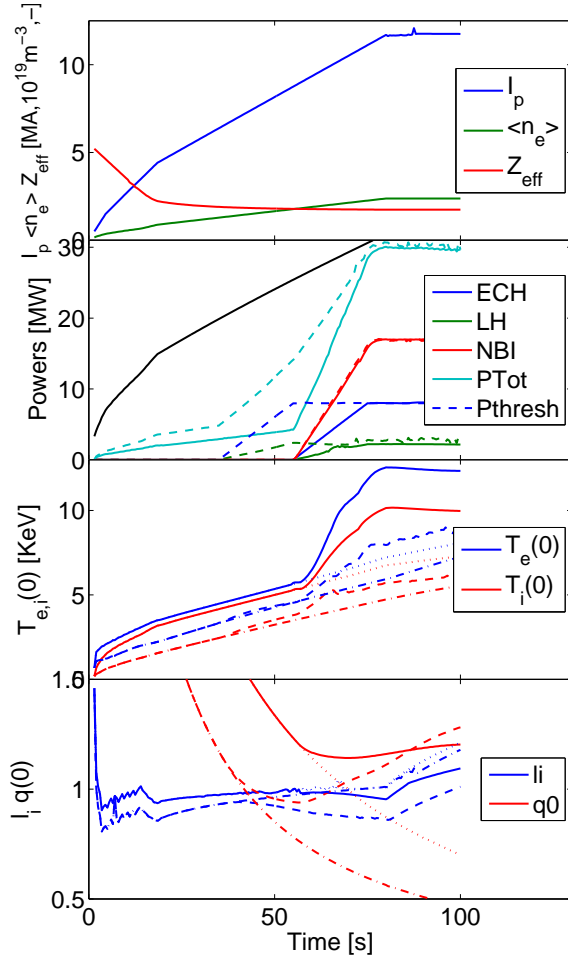


Figure 2: Time traces of the optimized scenario for the reference case, assuming scaling model (full lines) or Bohm-gyroBohm model (dashed lines). For comparison the figure also shows the time traces without any additional heating (dotted and dashed-dotted lines, respectively).

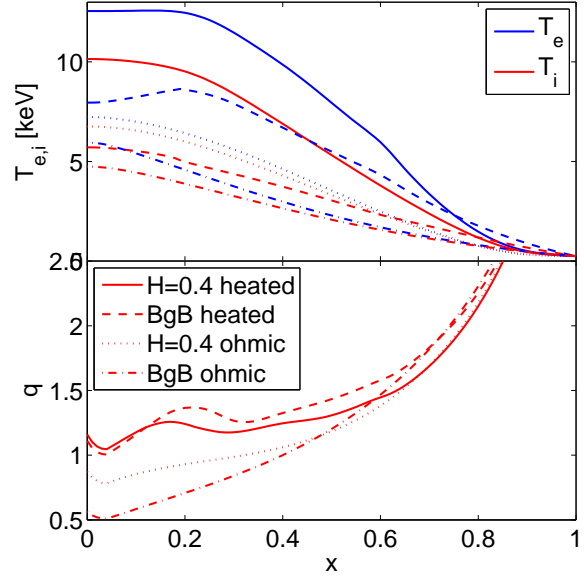


Figure 3:  $T_{e,i}$  and  $q$  profiles for the same cases and with the same line coding as the previous figure.

**5. Sensitivity analysis** Regarding sensitivity of the results to the assumptions, following parameters were varied:  $T_{e,i}$ (edge) (by 40%),  $n_e$  (by 60%),  $n_e$  profile shape (parabolic vs. flat) and  $Z_{\text{eff}}$ . We will only consider the scaling model ( $H=0.4$ ) here; the sensitivity of the simulations to these changes when using the Bohm/gyroBohm model is quite similar and can be accounted for in the same way.

(i) varying edge  $T_e$  gives only a modest change of  $l_i$  ( $\simeq 0.04$ ) and a tiny change of  $q$ , so poses no problem.

(ii)  $n_e$  peaking: The peaking of the  $T_e$  profile decreases with increasing peaking of  $n_e$ . Hence a flat / more peaked  $n_e$  profile will cause the current diffusion to be faster / slower. Indeed in an ITER ramp-up without additional heating, the time that  $q(0)$  reaches 1 ( $t(q_0 = 1)$ ) is shifted forward / backward by  $\sim 10$  s. This can be compensated for by a corresponding earlier / later start of the additional heating. See Fig.4.

(iii)  $Z_{\text{eff}}$ : A 40% higher/lower value of  $Z_{\text{eff}}$  causes a faster/slower current diffusion, and a shift of  $t(q_0 = 1)$  of  $\sim 10$  s, which can be compensated for like the previous case.

(iv)  $n_e$ : We only consider the effect of a 40% higher  $n_e$ . Again this causes (due to lower  $T_e$ ) faster current diffusion. Since now also  $P_{\text{LHthr}}$  is higher by  $\simeq 10$  MW, the applied power can be higher by this amount; moreover higher  $n_e$  allows earlier application of NBI. With the thus adapted heating scheme the flat  $q$  profile can be restored, and also  $l_i$  stays more on the safe side; see Figs.5 and 6.

**5. Conclusions and Outlook** The heating systems available at ITER allow, within the operational limits, the attainment of a hybrid  $q$  profile at the end of the current ramp-up. This is reached by a combination of NBI, ECCD (UPL) and LHCD.

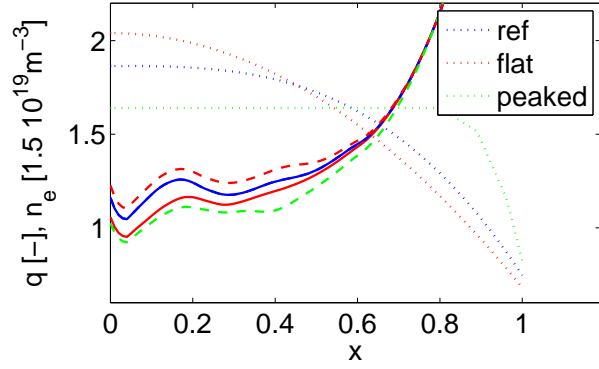


Figure 4: Effect of flat or extra peaked  $n_e$  profile. Plotted are  $n_e$  and  $q$  profiles at 80 s for the 3 cases (see legend), without (dashed lines) and with adapted heating scheme (full lines).

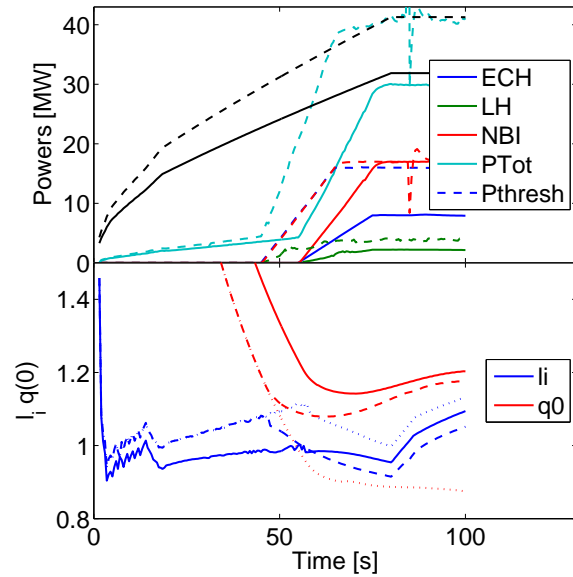


Figure 5: Time traces of reference case (full lines), high  $n_e$  case with the same heating scheme (dashed) and with adapted heating scheme (dotted).

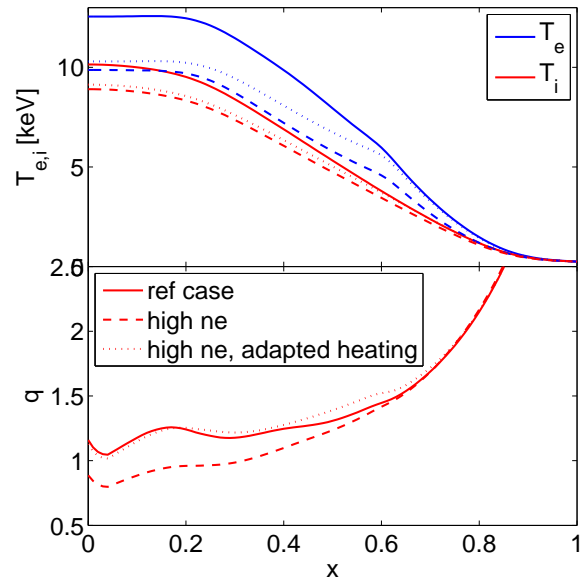


Figure 6: Profiles of  $T_{e,i}$  and  $q$  for the same cases as Fig.5.

The optimum heating scheme depends on chosen transport model. Moreover, modified assumptions on  $n_e$  peaking, edge  $T_{e,i}$  and  $Z_{\text{eff}}$  can be easily accounted for by a shift in time of the heating scheme. A higher density during the ramp-up phase can be accounted for equally well, and might even be profitable because it gives more freedom in the application of the heat sources.

Recently the ITER team is considering breakdown of the plasma at the HFS instead of on the LFS of the torus. This implies a different geometry in the very early phase of the discharge. The effect of this on the current density evolution, although it is expected to be small, will be considered in future sensitivity studies. Also the effect of faster  $I_p$  ramp will be the subject of further study.

## References

- [1] J. Citrin *et al*, *Nucl. Fusion* **50** (2010) 115007
- [2] G.M.D. Hogeweyj *et al*, Proc. 37th Eur. Conf., 2010, CD-ROM file P1.1041
- [6] I. Voitsekhovitch *et al*, *Plasma Phys. Contr. Fusion* **52** (2010) 105011
- [4] J.-F. Artaud *et al*, *Nucl. Fusion* **50** (2010) 043001
- [5] V. Lukash *et al*, *Plasma Devices and Oper.* **15** (2007) 283
- [6] H. Weisen *et al*, *Nucl. Fusion* **45** (2005) L1
- [7] ref FREEBIE

**Acknowledgements** This work, supported by the European Communities under the contract of Association between EURATOM/FOM, was carried out within the framework of the

European Fusion Programme with financial support from NWO. The views and opinions expressed herein do not necessarily reflect those of the European Commission. This work is supported by NWO-RFBR Centre-of-Excellence on Fusion Physics and Technology (Grant nr. 047.018.002).